Patch Antennas on Ferromagnetic Substrates

Arik Darnell Brown, John L. Volakis, *Fellow, IEEE,* Leo C. Kempel, *Member, IEEE,*
and Youssry Y. Botros

***Abstract*— Patch antennas on ferrite substrates allow for pattern control, frequency shifting, and scattering reduction. This is achieved by external magnetic field biasing coupled with the inherent magnetization of the ferrite substrate. Measurements and analytical studies based on the method of moments (MoM) have verified these attractive properties of ferrite substrates. However, verification of the analysis is difficult and, furthermore, previous models have relied on uniform biasing across the substrate. In this paper, we present a hybrid finite element-boundary integral (FE-BI) method, which permits modeling of the true nonuniform bias fields within the substrate for a more accurate prediction of the ferrite patch performance. After validation of the proposed simulation and a demonstration of the inherent properties of the ferrite patch, it is shown that nonuniform biasing is responsible for additional frequency shifts. We also identify the poor condition of the resulting matrix systems and relate this situation to the predictable occurrence of nonpropagating substrate modes. A more robust iterative solver with preconditioning is, therefore, proposed and applied to handle these situations.**

***Index Terms*— Anisotropic media, antennas, antenna theory, ferrites, finite-element methods, microstrip antennas.**

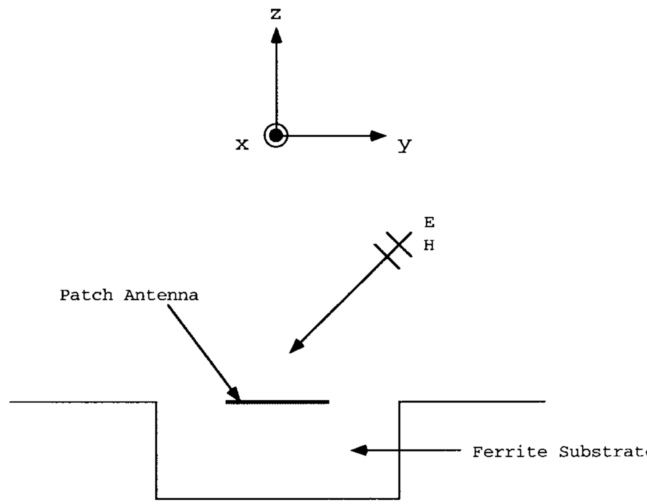

Fig. 1. Geometry for a patch antenna on an anisotropic substrate.

I. Introduction

PATCH antennas on ferrite substrates are attractive because they offer greater agility in controlling the radiation characteristics of the antenna. Their inherent anisotropy and nonreciprocal properties [1], permit variable frequency tuning [2]–[4], and antenna polarization diversity [5]. External biasing of the ferrite substrate also allows for beam steering [6]–[9], pattern shape control, and radar cross section control [10], [11] by forcing the ferrite into a cutoff state [12].

Several papers have already considered the performance of ferrite patch antennas. These works [13]–[16] employed the method of moments (MoM) technique in conjunction with the substrate Green's function. Validation of the results given in [14] and [16] have so far been difficult to achieve. Also, MoM formulations do not permit modeling of nonuniform biasing and inhomogeneous constitutive parameters, a situation that inherently occurs when the ferrite is biased. To provide for greater flexibility in modeling the ferrite substrate and the substrate cavity (see Fig. 1), we performed an analysis of the ferrite patch using the finite element-boundary integral (FE-BI) method. As usual, the substrate housed within the cavity is modeled by the finite-element method (FEM) using an edge-based formulation [17], [18]. Consequently, multiple substrate (and superstrate) layers can be handled easily including lateral material inhomogeneities within each layer. In our formulation, the FE mesh is truncated at the surface of the cavity using the rigorous BI method. Thus, the proposed FE-BI implementation is equally rigorous to the traditional MoM (employing the substrate Green's function) and allows modeling of finite and inhomogeneous substrates.

In the following sections, we first give a brief description of the formulation and it's implementation for ferrite materials. We then proceed with the presentation of some simple ferrite patch antenna calculations involving scattering and radiation examples. These serve to validate the implementation and preciseness of the results. They also reveal that serious solution convergence difficulties can arise for certain bias states of the substrate. It is shown that these difficulties can be predicted *a priori.* For our implementation we resorted to a more robust iterative solver, the generalized minimal residual method (GMRES) with preconditioning. Calculations showing the effects of biasing on the antenna resonance and scattering characteristics are given in the latter part of the paper. Our final example is a calculation simulating a nonuniform substrate (due to natural biasing). This example demonstrates the importance of modeling these nonuniformities accurately for evaluating the performance of the radiating element.

II. Formulation

The geometry to be considered (see Fig. 1) consists of a patch situated in a rectangular cavity. The presence of the cavity eliminates radiation loss via surface waves and does not affect the radiation pattern provided the cavity perimeter is placed at some small distance from the patch edges. To

Manuscript received November 6, 1997; revised June 15, 1998.

A. D. Brown, J. L. Volakis, and Y. Y. Botros are with the Radiation Laboratory, Department of Electrical Engineering and Computer Science, University of Michigan, Ann Arbor, MI 48109 USA.

L. C. Kempel was with the Mission Research Corporation, Valparaiso, FL. He is now with Michigan State University, East Lansing, MI 48823 USA.

Publisher Item Identifier S 0018-926X(99)02203-6.

obtain the unknown field in the context of FEM, the variational equation

$$\delta F(\mathbf{E}) = 0 \tag{1}$$

is solved [18], where

$$\begin{aligned} F(\mathbf{E}) = &\frac{1}{2} \iiint_V \left[\frac{1}{\mu_r}(\nabla \times \mathbf{E}) \cdot (\nabla \times \mathbf{E}) - k_o^2 \epsilon_r \mathbf{E}\mathbf{E}\right] dV \\ &+ \iiint_V \left[jk_o Z_o \mathbf{J}^{int} \cdot \mathbf{E} - \frac{1}{\mu_r}\mathbf{M}^{int} \cdot (\nabla \times \mathbf{E})\right] dV \\ &+ jk_o Z_o \iint_S (\mathbf{E} \times \mathbf{H}) \cdot \hat{z}\, dS. \end{aligned} \tag{2}$$

In this equation, V denotes the cavity volume, S is the cavity aperture, ϵ_r and μ_r are the relative permittivity and permeability of the ferrite substrate, $\mathbf{J}^{int}$ and $\mathbf{M}^{int}$ are internal electric and magnetic sources due to the antenna feeds, and the last term in (2) is the BI term. Discretization of (1) using Galerkin's method leads to the linear system

$$[A]\{E\} = \{B\} \tag{3}$$

where $[A]$ is an $N \times N$ matrix and $\{B\}$ is an $N \times 1$ column vector given by [17].

When modeling gyromagnetic substrates, the functional must be modified to incorporate the inherent anisotropy of the ferrite material. Specifically, for general anisotropic media we have

$$\begin{aligned} F(\mathbf{E}) = &\tfrac{1}{2} \iiint_V [\overline{\overline{\mu}}_r^{-1} \cdot (\nabla \times \mathbf{E}) \cdot (\nabla \times \mathbf{E}) - k_o^2 \overline{\overline{\epsilon}}_r \cdot \mathbf{E}\mathbf{E}]\, dV \\ &+ \iiint_V [jk_o Z_o \mathbf{J}^{int} \cdot \mathbf{E} - \frac{1}{\mu_r}\mathbf{M}^{int} \cdot (\nabla \times \mathbf{E})]\, dV \\ &+ jk_o Z_o \iint_S (\mathbf{E} \times \mathbf{H}) \cdot \hat{z}\, dS \end{aligned} \tag{4}$$

where $\overline{\overline{\epsilon}}_r$ and $\overline{\overline{\mu}}_r$ are the relative permittivity and Polder permeability tensors. The element matrices in the FE assembly process resulting from this functional are given in the Appendix.

For a z-biased ferrite $\overline{\overline{\mu}}_r$ is given by

$$\overline{\overline{\mu}} = \begin{pmatrix} \mu & j\kappa, & 0 \\ -j\kappa & \mu, & 0 \\ 0, & 0 & \mu_o \end{pmatrix} \tag{5}$$

and for other biasing directions (x and y) the tensor entries are simply rotated accordingly [1]. Here, the parameters μ and κ are functions of frequency given by

$$\mu = \mu_o\left(1 + \frac{\omega_o \omega_m}{\omega_o^2 - \omega^2}\right) \tag{6}$$

$$\kappa = \mu_o\left(\frac{\omega \omega_m}{\omega_o^2 - \omega^2}\right) \tag{7}$$

where

$$\omega_o = \gamma(\mu_o H_o) \tag{8}$$

and

$$\omega_m = \gamma(\mu_o M_s). \tag{9}$$

Also, M_s is the saturation magnetization, H_o is the dc bias field, γ is the gyromagnetic ratio, and ω_o and ω_m are the precession and forced precession frequencies, respectively.

When dealing with ferrite materials, the field behavior is determined by the propagation direction and its orientation with the applied magnetic bias field direction. There are two separate cases which determine the effective permeability (μ_{eff}) within the ferrite [1], [21]—the longitudinal case where propagation is parallel to the applied bias field and the transverse case where propagation is perpendicular to the applied bias field. In the longitudinal case

$$\mu_{\text{eff}} = \mu \pm \kappa \tag{10}$$

whereas in the transverse case

$$\mu_{\text{eff}} = \frac{\mu^2 - \kappa^2}{\mu}. \tag{11}$$

For both propagation modes, the propagation constant within the ferrite is calculated as

$$\gamma = j\omega\sqrt{\epsilon_o \epsilon_r \mu_o \mu_{\text{eff}}} \tag{12}$$

$$= \alpha + j\beta. \tag{13}$$

The modes due to the propagation constant play a major role in the FE solution.

Because of their tensor properties, ferrites introduce a great deal of complexity into the formulation when solving radiation problems. When using the FE method, it is observed that the system matrix becomes asymmetric and can be poorly conditioned at certain values of the ferrite parameters. Initially, the biconjugate gradient (BiCG) method was used for solving the matrix system. To improve performance, a preconditioned BiCG algorithm was also examined. However, the BiCG was not robust under certain bias conditions. In these cases, we resorted to the GMRES method as described later.

III. Applications and Validation

A. Probe-Fed Patch Antenna

Consider the probe-fed patch antenna geometry given in Fig. 1. For this example the ferrite substrate parameters were $4\pi M_s = 650$ G, $H_o = 600$ Oe, and $\epsilon_r = 10$. The calculated input impedance and radiation pattern are given in Figs. 2 and 3. As expected, biasing caused a shift in resonance and this is clearly seen in Fig. 2. Specifically, the ferrite substrate decreased the lowest resonance of the patch from 4.44 to 2.24 GHz, thus reducing the overall size of the patch for operation at the same frequency. From Fig. 3, we also observe that the biased patch exhibits a null along the horizontal direction. This patch was also considered by Schuster and Luebbers [19] using the finite-difference time-domain (FDTD) method. Our computed resonance shift was within 40 MHz of their values (1.8%). Although this type of agreement is considered very good for patch antennas, the small difference may be attributed to possible numerical implementation inaccuracies. Our simulation used a cavity size of 4.085 cm × 4.085 cm × 0.015 cm and the FE-BI system consisted of 3766 unknowns.

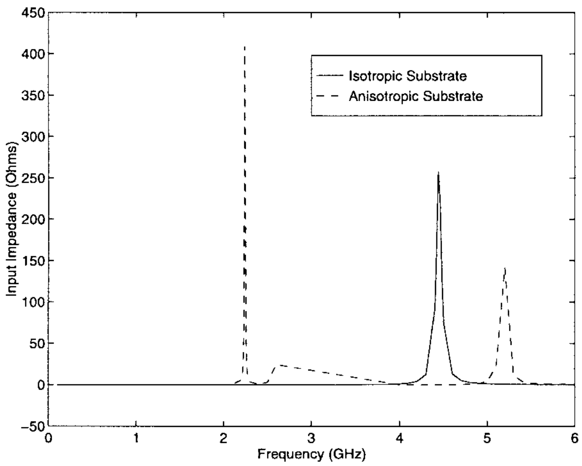

Fig. 2. Real input impedance.

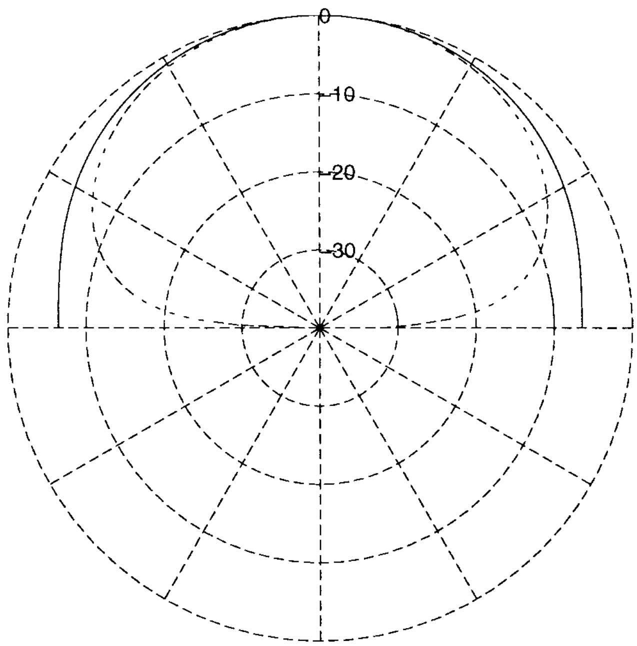

Fig. 3. Radiation pattern in the yz plane on an x-biased ferrite substrate (frequency = 2.2 GHz, — isotropic substrate, - - anisotropic substrate).

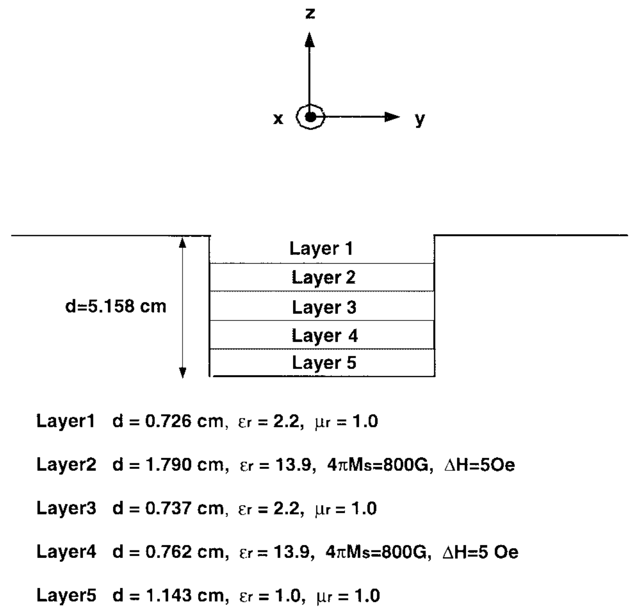

Fig. 4. Geometry of a cavity with ferrite layers.

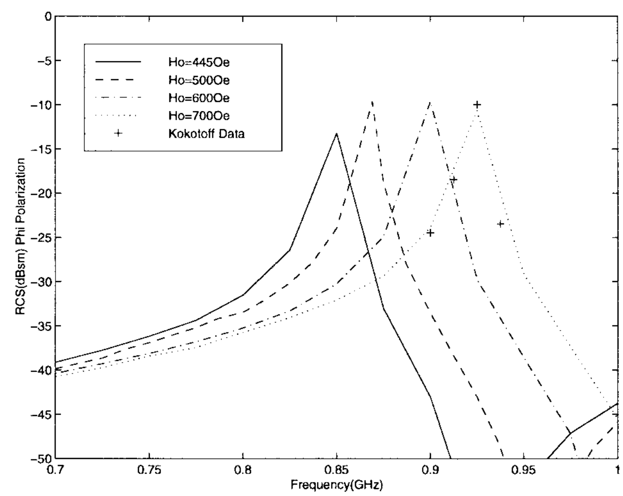

Fig. 5. Effect of biasing on the RCS of the cavity in Fig. 4. All computations were carried out using the FE-BI method except as noted.

B. Ferrite Filled Cavity

1) Biased Substrate: Consider now a cavity with several magnetized layers as shown in Fig. 4. Layers 2 and 4 are magnetized in the $\hat{\mathbf{y}}$ direction, e.g.,

$$\overline{\overline{\mu}}_r = \begin{pmatrix} \mu, & 0 & j\kappa \\ 0 & \mu_o, & 0 \\ -j\kappa, & 0 & \mu \end{pmatrix}. \tag{14}$$

This is a particular example considered by Kokotoff [20]. The radar cross section (RCS) of the layered ferrite cavity for different biasing values (H_o) is given in Fig. 5, and our calculations are seen to be in agreement to those of Kokotoff [20] for all cases.

This example again demonstrates the frequency shifting property of ferrite materials with biasing and validates the employed FEM formulation. The number of unknowns for this example was 6776 (BI unknowns = 420).

2) Unbiased Substrate: We next consider a three-layer cavity consisting of a ferrite layer between two free-space layers. The ferrite layer is magnetized with parameters $\epsilon_r = 13.9$ and $4\pi M_s = 800$ G. However, no biasing is applied. As shown in Fig. 7, calculations using the BiCG solver for $M_s = 0$ were in complete agreement with results given by Kokotoff. Fig. 8 shows results for the same geometry with the ferrite layer magnetized. About 780 unknowns (BI unknowns $\simeq 180$) were used to simulate this cavity. This example presented us with convergence difficulties when the BiCG solver was used. An investigation of several other cases demonstrated that, in general, convergence difficulties were encountered when the propagation constant β, as given in (13), was zero for one of the modes. For this example, β vanished for one of the longitudinal modes corresponding to $\mu_{\text{eff}} = \mu + \kappa$ and the transverse modes. The actual values of β for all three modes are given in Fig. 9 and we observe that for the aforementioned

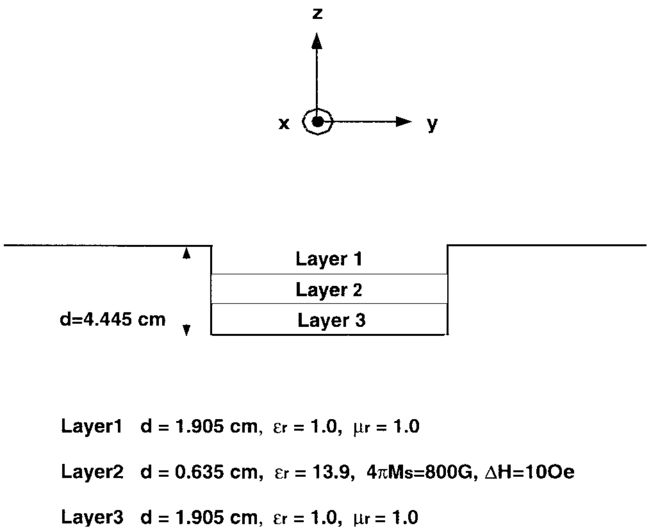

Fig. 6. Ferrite cavity geometry.

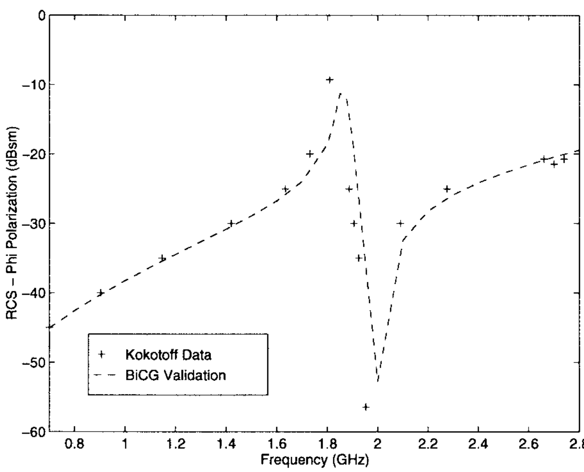

Fig. 7. RCS (normal incidence) using the FE-BI of the loaded cavity in Fig. 6, with $M_s = 0$ (i.e., no magnetization).

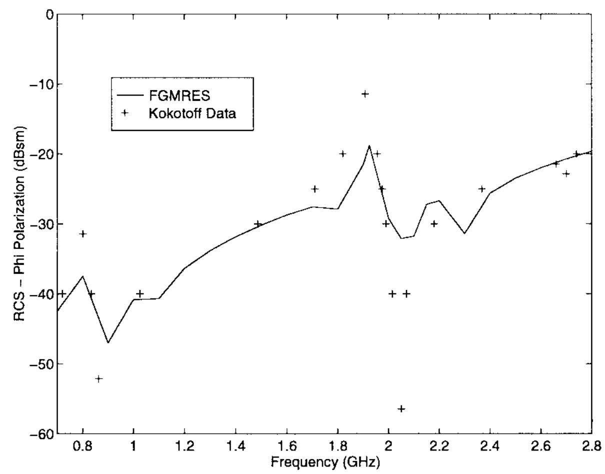

Fig. 8. RCS (normal incidence), using the FE-BI, of the loaded cavity shown in Fig. 6, with the values of M_s and ΔH as given there.

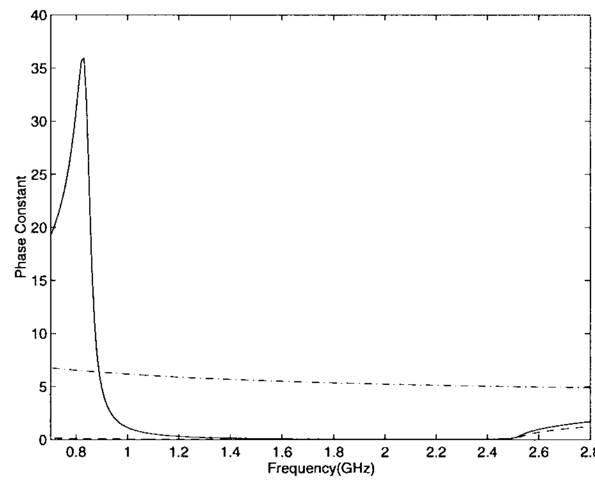

Fig. 9. β normalized to k_o, — $\mu_{\rm eff} = (\mu^2 - \kappa^2)/\mu$, - - $\mu_{\rm eff} = \mu + \kappa$, -.-.. $\mu_{\rm eff} = \mu - \kappa$ for a ferrite medium having $4\pi M_s = 800$ G, $\Delta H = 10$ Oe, and $\epsilon_r = 13.9$.

two modes, β vanishes from about 1–2.5 GHz (see Fig. 9). In concert, the BiCG solver failed to converge within this frequency range. Results based on a direct solver were also inaccurate due to the poor system condition. To overcome convergence difficulties for those frequencies where $\beta = 0$ for one or more of the modes, we resorted to a more robust iterative solver such as the preconditioned flexible GMRES (FGMRES) [22].

Features that made the FGMRES algorithm attractive were its guaranteed convergence, ability to adapt variable preconditioners, and a predictable error history (i.e., a smooth and monotonic convergence pattern as compared to the erratic convergence pattern of the BiCG algorithm). An important parameter for the GMRES solver is the number of interior iterations (m) before restarting the solver. These initial iterations control the number of spanning basis vectors used for an initial approximation of the solution. For our examples, the minimum m used was 70 while the maximum m was 280. For frequencies where the system is ill conditioned, a higher value for m is required along with preconditioning. From our analysis, these points occur near resonance, which is approximately 1.98 GHz (Fig. 8).

Using the GMRES solver, with the approximate inverse preconditioner (AIPC) [22], convergence was obtained at all points for the geometry in Fig. 6. Fig. 8 shows the results, and we observed that the GMRES solution tracks the data in [20] quite well. Given the poor condition of the system, it is not clear as to which of the curves in Fig. 8 is not accurate.

IV. Nonuniform Biasing

When building a ferrite antenna a permanent magnet is required to produce the applied magnetic bias field. Due to the finite nature of the magnet, the field is no longer uniform and, thus, the electrical material properties become inhomogeneous. Since many analysis methods assume a uniform bias field, this produces a solution which is no longer accurate. In contrast, the FEM allows for arbitrary specification of the material within the volume, which is an inherent advantage of FEM over other numerical methods.

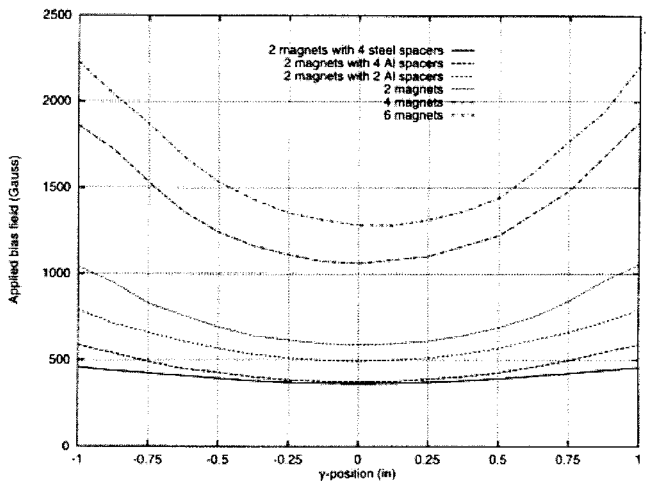

Fig. 10. Measurement of the nonuniform magnetic field within a cavity.

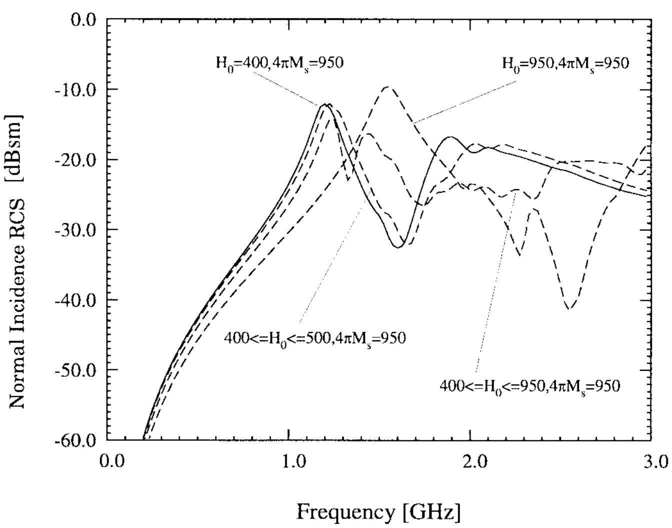

Fig. 11. RCS due to a nonuniform magnetic field (see Fig. 10) across a 6 cm × 6 cm × 1 cm cavity.

To observe the effect of nonuniform magnetization, let us consider the modeling of the measured bias field in a ferrite cavity as given in Fig. 10 [20]. Indeed, Fig. 10 reveals a difference of more than 1000 G at different locations within the cavity, showing the necessity of the FEM technique to handle this inhomogeneous behavior. RCS calculations for this nonuniform biasing are provided in Fig. 11 for a 6 cm × 6 cm × 1 cm cavity filled with this material. It is clear, that the resonance of the cavity is substantially affected by the nonuniformity of the bias field.

V. Conclusion

In this paper, we presented several results and validations demonstrating the attractive properties of ferrite patch antennas. The high dielectric constant of the ferrite, inherent magnetization, and external biasing all serve to minimize the size of the patch, in addition to providing pattern control and lower radar cross section over a given band. The employed hybrid FE-BI method also permitted an investigation on the effects of the typical nonuniform bias fields that occur across the substrate volume. These nonuniform bias fields cause inhomogeneities that affect the operation frequency and overall response of the antenna and may be a cause of discrepancies between measurements and calculations. Our study also showed that poor matrix conditions and solution convergence difficulties may be traced to band regions where one or more ferrite modes are nonpropagating. This situation prompted the use of more robust iterative solvers, and, to achieve convergence, a preconditioned version of the GMRES method was used. GMRES proved effective in cases where the usual conjugate and biconjugate gradient algorithms failed.

Appendix
Anisotropic Formulation

In the FEM formulation, the relevant integrals to be computed in the volume domain are

$$\mathbf{E}_{ij}^e = \iiint_{V_e} \nabla \times \mathbf{N}_i \cdot (\overline{\overline{\mu}}_r^{-1} \cdot \nabla \times \mathbf{N}_j)\, dV_e \tag{15}$$

$$\mathbf{F}_{ij}^e = \iiint_{V_e} \mathbf{N}_i \cdot (\overline{\overline{\epsilon}}_r \cdot \mathbf{N}_j)\, dV_e \tag{16}$$

where

$$\overline{\overline{\mu}}_r^{-1} = \begin{pmatrix} \tilde{\mu}_{xx} & \tilde{\mu}_{xy} & \tilde{\mu}_{xz} \\ \tilde{\mu}_{yx} & \tilde{\mu}_{yy} & \tilde{\mu}_{yz} \\ \tilde{\mu}_{zx} & \tilde{\mu}_{zy} & \tilde{\mu}_{zz} \end{pmatrix} \tag{17}$$

$$\overline{\overline{\epsilon}}_r = \begin{pmatrix} \epsilon_{xx} & \epsilon_{xy} & \epsilon_{xz} \\ \epsilon_{yx} & \epsilon_{yy} & \epsilon_{yz} \\ \epsilon_{zx} & \epsilon_{zy} & \epsilon_{zz} \end{pmatrix} \tag{18}$$

$$\mathbf{E}^e = \begin{pmatrix} \mathbf{E}_{xx} & \mathbf{E}_{xy} & \mathbf{E}_{xz} \\ \mathbf{E}_{yx} & \mathbf{E}_{yy} & \mathbf{E}_{yz} \\ \mathbf{E}_{zx} & \mathbf{E}_{zy} & \mathbf{E}_{zz} \end{pmatrix} \tag{19}$$

and

$$\mathbf{F}^e = \begin{pmatrix} \mathbf{F}_{xx} & \mathbf{F}_{xy} & \mathbf{F}_{xz} \\ \mathbf{F}_{yx} & \mathbf{F}_{yy} & \mathbf{F}_{yz} \\ \mathbf{F}_{zx} & \mathbf{F}_{zy} & \mathbf{F}_{zz} \end{pmatrix}. \tag{20}$$

The values for the brick-element matrices in a general anisotropic medium are

$$\mathbf{K}_1 = \begin{pmatrix} 2 & -2 & 1 & -1 \\ -2 & 2 & -1 & 1 \\ 1 & -1 & 2 & -2 \\ -1 & 1 & -2 & 2 \end{pmatrix} \tag{21}$$

$$\mathbf{K}_2 = \begin{pmatrix} 2 & 1 & -2 & -1 \\ 1 & 2 & -1 & -2 \\ -2 & -1 & 2 & 1 \\ -1 & -2 & 1 & 2 \end{pmatrix} \tag{22}$$

$$\mathbf{K}_3 = \begin{pmatrix} -1 & -1 & 1 & 1 \\ 1 & 1 & -1 & -1 \\ -1 & -1 & 1 & 1 \\ 1 & 1 & -1 & -1 \end{pmatrix} \tag{23}$$

$$\mathbf{K}_4 = \begin{pmatrix} 1 & -1 & 1 & -1 \\ -1 & 1 & -1 & 1 \\ 1 & -1 & 1 & -1 \\ -1 & 1 & -1 & 1 \end{pmatrix} \tag{24}$$

$$\mathbf{K}_5 = \begin{pmatrix} 2 & 1 & -2 & -1 \\ -2 & -1 & 2 & 1 \\ 1 & 2 & -1 & -2 \\ -1 & -2 & 1 & 2 \end{pmatrix} \tag{25}$$

$$\mathbf{K}_6 = \begin{pmatrix} 1 & 1 & -1 & -1 \\ 1 & 1 & -1 & -1 \\ -1 & -1 & 1 & 1 \\ -1 & -1 & 1 & 1 \end{pmatrix} \tag{26}$$

$$\mathbf{E}_{xx} = \frac{l_x l_z \tilde{\mu}_{zz}}{6 l_y}\mathbf{K}_1 + \frac{l_x l_y \tilde{\mu}_{yy}}{6 l_z}\mathbf{K}_2 + \frac{l_x \tilde{\mu}_{zy}}{4}\mathbf{K}_3 + \frac{l_x \tilde{\mu}_{yz}}{4}\mathbf{K}_3^T \tag{27}$$

$$\mathbf{E}_{yy} = \frac{l_x l_y \tilde{\mu}_{xx}}{6 l_z}\mathbf{K}_1 + \frac{l_y l_z \tilde{\mu}_{zz}}{6 l_x}\mathbf{K}_2 + \frac{l_y \tilde{\mu}_{xz}}{4}\mathbf{K}_3 + \frac{l_y \tilde{\mu}_{zx}}{4}\mathbf{K}_3^T \tag{28}$$

$$\mathbf{E}_{zz} = \frac{l_y l_z \tilde{\mu}_{yy}}{6 l_x}\mathbf{K}_1 + \frac{l_x l_z \tilde{\mu}_{xx}}{6 l_y}\mathbf{K}_2 + \frac{l_z \tilde{\mu}_{yx}}{4}\mathbf{K}_3 + \frac{l_z \tilde{\mu}_{xy}}{4}\mathbf{K}_3^T \tag{29}$$

$$\mathbf{E}_{xy} = \frac{-l_z \tilde{\mu}_{zz}}{6}\mathbf{K}_5 + \frac{l_x \tilde{\mu}_{zx}}{4}\mathbf{K}_4 + \frac{l_y \tilde{\mu}_{yz}}{4}\mathbf{K}_6 + \frac{l_x l_y \tilde{\mu}_{yx}}{4 l_z}\mathbf{K}_3^T \tag{30}$$

$$\mathbf{E}_{xz} = \frac{-l_y \tilde{\mu}_{yy}}{6}\mathbf{K}_5^T + \frac{l_x l_z \tilde{\mu}_{zx}}{4 l_y}\mathbf{K}_3 + \frac{l_z \tilde{\mu}_{zy}}{4}\mathbf{K}_4 + \frac{l_x \tilde{\mu}_{yx}}{4}\mathbf{K}_6 \tag{31}$$

$$\mathbf{E}_{yz} = \frac{-l_x \tilde{\mu}_{xx}}{6}\mathbf{K}_5 + \frac{l_y l_z \tilde{\mu}_{zy}}{4 l_x}\mathbf{K}_3 + \frac{l_y \tilde{\mu}_{xy}}{4}\mathbf{K}_4 + \frac{l_z \tilde{\mu}_{zx}}{4}\mathbf{K}_6 \tag{32}$$

$$\mathbf{F}_{ij} = \frac{l_x l_y l_z \epsilon_{xy}}{36}\begin{pmatrix} 4 & 2 & 2 & 1 \\ 2 & 4 & 1 & 2 \\ 2 & 1 & 4 & 2 \\ 1 & 2 & 2 & 4 \end{pmatrix}; \qquad i = j,\ i = x,\ y,\ z \tag{33}$$

$$\mathbf{L}_1 = \begin{pmatrix} 2 & 1 & 2 & 1 \\ 2 & 1 & 2 & 1 \\ 1 & 2 & 1 & 2 \\ 1 & 2 & 1 & 2 \end{pmatrix} \tag{34}$$

$$\mathbf{F}_{xy} = \frac{l_x l_y l_z \epsilon_{xy}}{24}\mathbf{L}_1 \tag{35}$$

$$\mathbf{F}_{yx} = \frac{l_x l_y l_z \epsilon_{yx}}{24}\mathbf{L}_1^T \tag{36}$$

$$\mathbf{F}_{xz} = \frac{l_x l_y l_z \epsilon_{xz}}{24}\mathbf{L}_1^T \tag{37}$$

$$\mathbf{F}_{zx} = \frac{l_x l_y l_z \epsilon_{zx}}{24}\mathbf{L}_1 \tag{38}$$

$$\mathbf{F}_{yz} = \frac{l_x l_y l_z \epsilon_{yz}}{24}\mathbf{L}_1 \tag{39}$$

$$\mathbf{F}_{zy} = \frac{l_x l_y l_z \epsilon_{zy}}{24}\mathbf{L}_1^T. \tag{40}$$

REFERENCES

[1] D. M. Pozar, *Microwave Engineering.* Reading, MA: Addison-Wesley, 1996.

[2] P. J. Rainville and F. J. Harackiewiz, "Magnetic tuning of a microstrip patch antenna fabricated on a ferrite film," *IEEE Microwave Guided Wave Lett.*, vol. 2, p. 483–485, Dec. 1992.

[3] H. How and C. Vittoria, "Radiation frequencies of ferrite patch antennas," *IEEE Electron. Lett.*, vol. 28, no. 15, pp. 1405–1406, 1992.

[4] D. M. Pozar and V. Sanchez, "Magnetic tuning of a microstrip antenna on a ferrite substrate," *Electron. Lett.*, vol. 24, no. l2, pp. 729–731, 1988.

[5] J. S. Roy, P. Vaudon, A. Reineix, F. Jecko, and B. Jecko, "Circularly polarized far fields of an axially magnetized circular ferrite microstrip antenna," *Microwave Opt. Tech. Lett.*, vol. 5, pp. 228–230, 1992.

[6] N. Okamoto and S. Ikeda, "An experimental study of electronic scanning by an antenna loaded with a circular array of ferrite rods," *IEEE Trans. Antennas Propagat.*, vol. AP-27, pp. 426–430, Dec. 1979.

[7] D. Guan, "Magnetic ferrite patch antenna array," *IEEE Trans. Magn.*, vol. 30, no. 6, pp. 4551–4553, Nov. 1994.

[8] N. Buris, T. B. Funk, and R. S. Silverstein, "Dipole arrays printed on ferrite substrates," *IEEE Trans. Antennas Propagat.*, vol. 41, pp. 165–175, Feb. 1993.

[9] H. Maheri, M. Tsutsumi, and N. Kumagai, "Experimental studies of magntically scannable leaky-wave antennas having a corrugated ferrite slab/dielectric layer structure," *IEEE Trans. Antennas Propagat.*, vol. 36, pp. 911–917, July 1988.

[10] A. Henderson and J. R. James, "Magnetized microstrip antenna with pattern control," *Electron. Lett.*, vol. 24, no. 1, pp. 45–47, 1988.

[11] D. M. Pozar, "Radar cross-section of microstrip antenna on normally biased ferrite substrate," *Electron. Lett.*, vol. 25, no. 16, pp. 1079–1080, 1989.

[12] ——, "RCS reduction for a microstrip antenna using a normally biased ferrrite substrate," *IEEE Microwave Guided Wave Lett.*, vol. 2, pp. 196–198, May 1992.

[13] H. Y. Yang, "Characteristics of switchable ferrite microstrip antennas," *IEEE Trans. Antennas Propagat.*, vol. 44, pp. 1127–1132, Aug. 1996.

[14] H. Y. Yang, J. A. Castaneda, and N. G. Alexopoulos, "The RCS of a microstrip patch on an arbitrarily biased ferrite substrate," *IEEE Trans. Antennas Propagat.*, vol. 41, pp. 1610–1614, Dec. 1993.

[15] B. Lee and F. J. Harackiewicz, "The RCS of a microstrip antenna on an in-plane biased ferrite substrate," *IEEE Trans. Antennas Propagat.*, vol. 44, pp. 208–211, Feb. 1996.

[16] D. M. Pozar, "Radiation and scattering characteristics of microstrip antennas on normally biased ferrite substrates," *IEEE Trans. Antennas Propagat.*, vol. 40, pp. 1084–1092, Sept. 1992.

[17] J. Jin and J. L. Volakis, "A hybrid finite element method for scattering and radiation by microstrip patch antennas and arrays residing in a cavity," *IEEE Trans. Antennas Propagat.*, vol. 39, pp. 1598–1604, Nov. 1991.

[18] J. L. Volakis, T. Özdemir, and J. Gong, "Hybrid finite element methodologies for antennas and scattering," *IEEE Trans. Antennas Propagat.*, vol. 45, pp. 493–507, Mar. 1997.

[19] J. Schuster and R. Luebbers, "FDTD for three-dimensional propagation in a magnetized ferrite," *IEEE Trans. Antennas Propagat.*, vol. 44, pp. 1648–1651, July 1996.

[20] D. M. Kokotoff, "Full wave analysis of a ferrite-tuned cavity-backed slot antenna," Ph.D. dissertation, Arizona State Univ., Tempe, AZ, 1995.

[21] H. How, T. Fang, and C. Vittoria, "Intrinsic modes of radiation in ferrite patch antennas," *IEEE Trans. Magn.*, vol. 42, no. 6, p. 988–994, June 1994.

[22] Y. Saad, *Iterative Methods for Sparse Linear Systems.* Boston, MA: PWS, 1996.

Arik Darnell Brown was born in Battle Creek, MI, on July 18, 1972. He received the B.S. degree in electrical engineering from the Massachusetts Institute of Technology, Cambridge, MA, in 1993, and the M.S. degree, in electrical engineering from the University of Michigan, Ann Arbor, in 1995. He is currently working toward the Ph.D. degree in the area of electromagnetics at the Radiation Laboratory, University of Michigan, Ann Arbor.

His current research interest is in the numerical modeling of ferrite antennas.

John L. Volakis (S'77–M'82–SM'89–F96) was born on May 13, 1956, in Chios, Greece. He received the B.E. degree (*summa cum laude*) from Youngstown State University, Youngstown, OH, in 1978, and the M.Sc. and Ph.D. degrees from the Ohio State University, Columbus, in 1979 and 1982, respectively.

Since 1984, he has been with the University of Michigan, Ann Arbor, where he is now a Professor in the Department of Electrical Engineering and Computer Science (EECS). From 1982 to 1984, he was with Rockwell International, Aircraft Division, El Segundo, CA, and from 1978 to 1982, he was a Graduate Research Associate at the Ohio State University ElectroScience Laboratory. Dr. Volakis has published about 140 articles in major refereed journal articles, more than 140 conference papers, several book chapters on numerical methods, and has coauthored two books: *Approximate Boundary Conditions in Electromagnetics* (London, U.K.: Institute of Electrical Engineers, 1995) and *Finite Element Method for Electromagnetics* (Piscataway, NJ: IEEE Press, 1998). Along with his students, he develops prototype algorithms for modeling antennas, radar scattering and imaging of aircraft structures, and microwave circuits. His primary research deals with the development and application of analytical and numerical techniques to large-scale scattering, printed antennas, and bioelectromagnetics.

Dr. Volakis served as an Associate Editor of the IEEE TRANSACTIONS ON ANTENNAS AND PROPAGATION from 1988 to 1992 and of *Radio Science* from 1994 to 1998. He chaired the 1993 IEEE Antennas and Propagation Society Symposium and Radio Science Meeting, Ann Arbor, MI, and is a current member of the AdCom for the IEEE Antennas and Propagation Society. He now serves as Associate Editor for the *Journal of Electromagnetic Waves and Applications* and the *IEEE Antennas and Propagation Society Magazine*. In 1998 he received the University of Michigan College of Engineering Research Excellence Award. He is a member of Sigma Xi, Tau Beta Pi, Phi Kappa Phi, and Commission B of URSI.

Leo C. Kempel (S'89–M'94) received the B.S.E.E. degree from the University of Cincinnati, Cincinnati, OH, in 1989 and the M.S.E.E. and Ph.D. degrees from the University of Michigan, Ann Arbor, in 1990 and 1994, respectively.

He is currently an Assistant Professor in the Department of Electrical Engineering at Michigan State University, East Lansing, where he is actively conducting research in hybrid methods, especially as applied to conformal antenna analysis and design. He was a Senior Engineer at Mission Research Corporation from 1994 to 1998. In that position, he led a team of investigators responsible for development in the area of computational electromagnetics, conformal antenna design, high-power microwave analysis, and other related sites. He is a coauthor of *Finite Element Method of Electromagnetics* (Piscataway, NJ: IEEE, 1998) and has published in the general areas of scattering and antenna analysis and design.

Dr. Kempel is a member of Eta Kappa Nu and Tau Beta Pi.

Youssry Y. Botros was born in Alexandria, Egypt, on May 1968. He received the B.Sc. and M.S. degrees from the Electrical Engineering Department, Alexandria University, in 1990 and 1993, respectively, and the Ph.D. degree from the Electrical Engineering and Computer Science Department at the University of Michigan, Ann Arbor, in 1998.

From 1990 to 1994, he worked as a Teaching and Research Assistant with the Electrical Engineering Department, Alexandria University. In 1995, he joined the Radiation Laboratory of the Electrical Engineering and Computer Science Department at the University of Michigan where he held Teaching and Research Assistant positions in the department. His research interests are in noninvasive cancer ablation using high-intensity focused ultrasound, inverse scattering, and numerical modeling for microwave circuits.